CHEMISTRY
A EUROPEAN JOURNAL

FULL PAPER

DOI: 10.1002/chem.201103419

# Quadracyclic Adenine: A Non-Perturbing Fluorescent Adenine Analogue

**Anke Dierckx,[a] Francois-Alexandre Miannay,[a] Nouha Ben Gaied,[b] Søren Preus,[c] Markus Björck,[a] Tom Brown,[b] and L. Marcus Wilhelmsson*[a]**

**Abstract:** Fluorescent-base analogues (FBAs) comprise a group of increasingly important molecules for the investigation of nucleic acid structure and dynamics as well as of interactions between nucleic acids and other molecules. Here, we report on the synthesis, detailed spectroscopic characterisation and base-pairing properties of a new environment-sensitive fluorescent adenine analogue, quadracyclic adenine (qA). After developing an efficient route of synthesis for the phosphoramidite of qA it was incorporated into DNA in high yield by using standard solid-phase synthesis procedures. In DNA qA serves as an adenine analogue that preserves the B-form and, in contrast to most currently available FBAs, maintains or even increases the stability of the duplex. We demonstrate that, unlike fluorescent adenine analogues, such as the most commonly used one, 2-aminopurine, and the recently developed triazole adenine, qA shows highly specific base-pairing with thymine. Moreover, qA has an absorption band outside the absorption of the natural nucleobases (>300 nm) and can thus be selectively excited. Upon excitation the qA monomer displays a fluorescence quantum yield of 6.8% with an emission maximum at 456 nm. More importantly, upon incorporation into DNA the fluorescence of qA is significantly less quenched than most FBAs. This results in quantum yields that in some sequences reach values that are up to fourfold higher than maximum values reported for 2-aminopurine. To facilitate future utilisation of qA in biochemical and biophysical studies we investigated its fluorescence properties in greater detail and resolved its absorption band outside the DNA absorption region into distinct transition dipole moments. In conclusion, the unique combination of properties of qA make it a promising alternative to current fluorescent adenine analogues for future detailed studies of nucleic acid-containing systems.

**Keywords:** DNA · DNA solid-phase synthesis · duplex stability · fluorescence · fluorescent adenine analogue

## Introduction

Fluorescence is an invaluable tool for researchers studying the structure and dynamics of nucleic acids and their interactions with other biomolecules. The main advantage of fluorescence over other standard techniques, such as X-ray crystallography, NMR spectroscopy, and electrophoresis, is its high sensitivity, versatility as well as the ability to monitor the dynamics of DNA/RNA. However, the use of fluorescence to study nucleic acids requires some form of labelling with a fluorescent marker since the natural nucleobases are virtually non-fluorescent ($\Phi_f \sim 10^{-4}$).[1] For this reason, there is an ongoing effort to develop different types of fluorescent probes with properties suited for various purposes. Most available dyes are tethered covalently to the nucleic acids by a linker, for example, fluorescein, rhodamine, the Alexa-dyes and the Cy-dyes. Since these fluorophores reside outside of the base stack, these are referred to as external modifications. A second class, namely internal modifications, comprise fluorescent nucleic acid base analogues (FBAs).[2] These molecules resemble one of the natural nucleobases, show at least some base pairing to one of the natural bases through hydrogen bonds, do not seriously perturb the natural DNA or RNA structure, and most importantly, are significantly fluorescent. Having the fluorescent probe inside the base stack has prominent advantages compared to externally attached bulky adducts, which can significantly perturb the DNA duplex structure and also interfere with the interaction with other molecules. Furthermore, FBAs in contrast to external probes, can be firmly stacked and hence report on the local structure and dynamics of the DNA duplex rather than the dynamics of the probe moiety itself.

[a] A. Dierckx,[+] Dr. F.-A. Miannay,[+] M. Björck, Prof. Dr. L. M. Wilhelmsson
Department of Chemical and Biological Engineering
Physical Chemistry, Chalmers University of Technology
41296 Gothenburg (Sweden)
Fax: (+46) 31-772-3858
E-mail: marcus.wilhelmsson@chalmers.se

[b] Dr. N. Ben Gaied, Prof. Dr. T. Brown
School of Chemistry, University of Southampton
SO17 1BJ Southampton (UK)

[c] S. Preus
Department of Chemistry, University of Copenhagen
Universitetsparken 5, 2100 Copenhagen (Denmark)

[+] These authors contributed equally to this work.

Supporting information for this article is available on the WWW under http://dx.doi.org/10.1002/chem.201103419.

Over recent decades several research groups have focused on the development of FBAs with the above-mentioned properties. However, synthesising the optimal FBA has proved challenging. Instead, each class of FBA holds specific advantages depending on the kind of experiment one wants to perform. Further development and characterisation of novel FBAs will hopefully lead to a more complete understanding of the relationship between their structural and fluorescence properties.[3] The base-discriminating analogues designed by Saito and co-workers,[4] the pyrimidine analogues designed by Tor et al.[5] and the cytosine analogue pyrrolo dC[6] as well as its derivatives[7] are just a few examples of thoroughly studied FBAs. Other classes, such as the pteridines designed by Hawkins et al. comprise the guanine analogues 3-MI[8] and 6-MI and the adenine analogues 6-MAP and DMAP[9] as their most promising members.[10] The size-expanded DNA alphabet designed by Kool et al. seems practical for evaluating steric effects in DNA duplex structures among other things.[11] Another unique group of FBAs is the tricyclic cytosine analogues tC and $tC^O$, the emission of which is virtually insensitive to their microenvironment.[12] In addition $tC^O$, together with the non-emissive cytosine analogue $tC_{nitro}$ have been shown to function as the first nucleobase FRET pair, and yield detailed distance and orientation information about the DNA duplex.[13] In contrast to this latter class, all other FBAs show sensitivity to their immediate surroundings.

One of the most popular and widely applied FBAs is the adenine analogue 2-aminopurine (2-AP). The high quantum yield as a monomer in water (0.68) is decreased dramatically upon incorporation into nucleic acids.[14] This sensitivity of the emission to the microenvironment has been successfully used in many applications, of which some examples are given below. Even though it has found use in numerous studies, 2-AP causes a moderate destabilisation of the DNA duplex.[15] Furthermore, it shows base-pairing to both thymine and cytosine and hence is not an ideal adenine analogue.[16] It also shows a considerable amount of dynamics inside DNA.[17] These properties can be a substantial drawback in studies requiring a high level of detail and a low level of perturbation to the DNA duplex.

Of the numerous studies involving FBAs over the past decades, only a few will be highlighted here to illustrate the importance of these fluorophores (for more examples see recent reviews by Sinkeldam et al.[2b] and Wilhelmsson et al.[2a]). Many applications involve the use of the change in emission upon interaction of another molecule with DNA or RNA. This can yield information on conformational changes both in the protein and the DNA/RNA. An illustration is the elegant study of the kinetics of promoter binding and open complex formation upon interaction of bacteriophage T7 RNA polymerase with DNA containing 2-AP modified promoters.[18] Another example, which generated information on the dissociation of the multimeric form of the HIV-1 integrase complex upon binding to DNA, involves the guanine analogue 3-MI.[19] Other applications focus on the structure of the DNA itself instead of interactions with other molecules. For instance the fluorescent adenosine analogue 6MAP has been used to analyse the pre-melting transitions of DNA A tracts.[20] FBAs are now also starting to appear in the field of nanotechnology. A first report of this involves the cytosine analogue $tC^O$ sensing the local stability of self-assembling DNA hexagons.[21] Finally, FBAs are also finding applications in the RNA field. This is nicely illustrated by the use of 2-AP as a probe for research on small RNAs and RNA elements that control gene expression.[22]

Here we present the detailed and optimised experimental procedure for the synthesis of the new fluorescent adenine analogue, quadracyclic adenine (qA, Figure 1). The synthesis

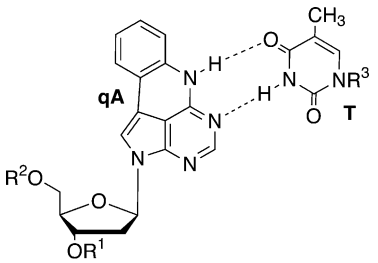


Figure 1. Structure of the qA monomer in the putative qA–T base pair. Measurements on the qA monomer were performed with $R^1=R^2=H$. For qA–T incorporated into DNA, $R^1$, $R^2$ and $R^3$ represent the rest of the DNA structure.

of qA (the 2′-deoxyriboside of 2,6-dihydro-2,3,5,6-tetraazaaceanthrylene; β anomer) has been reported by Matteucci et al. but no experimental procedure or analytical data were described.[23] Furthermore, we have found this nucleobase analogue to be emissive and therefore we now report on its fluorescent properties and present a detailed photophysical characterisation of qA both as a monomer and as a constituent of single- and double-stranded DNA. As a monomer, qA shows a lowest energy absorption band well-resolved from the natural DNA bases and we have located the transition dipole moments over this absorption band. Surprising results were obtained when investigating the quantum yields upon exciting over these different absorption transitions. Furthermore, we find that qA is moderately fluorescent as a monomer in water ($\Phi_f=6.8\,\%$, $\lambda_{ex}=337$ nm) compared to other adenine analogues, such as 2-AP.[14] However, upon incorporation into DNA, quantum yields reach maximum values, which are higher than those corresponding to 2-AP.[14] We also report on the non-perturbing properties of qA in DNA duplex systems. On average qA slightly stabilises DNA duplexes and CD measurements suggest that the DNA duplex adopts the B-form. Furthermore, qA is a selective adenine analogue since it shows specific base pairing to thymine only, in contrast to other fluorescent adenine analogues, such as 2-AP and triazole adenine.[16,24] To the best of our knowledge qA is the only fluorescent adenine analogue with such favourable properties.

  

## Results and Discussion

**Synthesis of the quadracyclic 2′-deoxyadenosine analogue, qA**: The synthesis of the quadracyclic analogue of 2′-deoxyadenosine (qA; 2′-deoxyriboside of 2,6-dihydro-2,3,5,6-tetraazaaceanthrylene; β anomer) has previously been reported by Matteucci et al. but no experimental procedures were described.[23] Here we report the synthesis of the corresponding phosphoramidite monomer (Scheme 1) and oligonucleotides containing qA (see the Supporting Information).

The synthesis of the qA phosphoramidite (**8**) was initiated with the conversion of the 2′-deoxyribose into 3,5-ditoluoyl-1-chloro-deoxyribose (predominantly α anomer; **1**)[25] in three steps with an overall yield of 36% (Scheme 1). Condensation of 6-chloro-7-deaza-7-iodopurine with the chloro sugar by using sodium hydride[26] gave the desired compound (**2**) in 73% yield. The major isomer was consistent with the β anomer by using proton NMR spectroscopy. Moreover, the final product that was later incorporated into oligonucleotides gave stable duplexes, further confirming the correct isomer. The sugar–base condensation step was followed by a Stille coupling. In the original work Matteucci et al.[23] used trimethylstannyl-*N*-(Boc)aniline obtained by *ortho*-functionalisation of the *N*-(Boc)aniline.[27] In our hands this step was low yielding and we attempted to overcome this problem using tributyltin chloride. Our first attempts, following the original procedure, gave very low yields and changing the catalyst, the solvent and the temperature did not improve the situation.

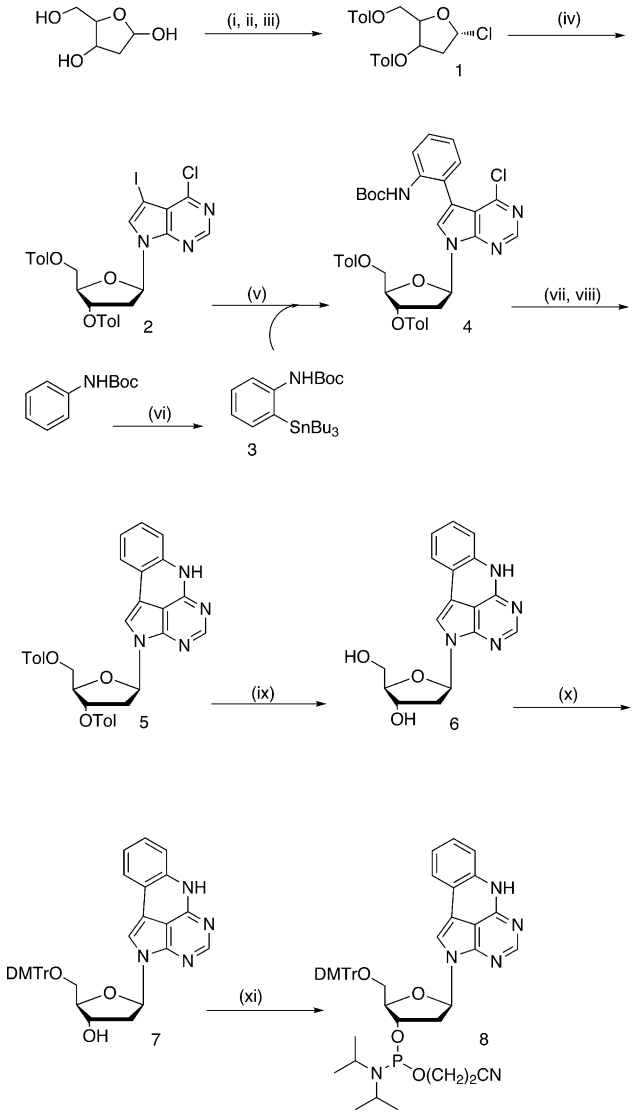


Scheme 1. Synthesis of the fluorescent quadracyclic phosphoramidite monomer (**8**). i) acetyl chloride, MeOH; ii) ρ-toluoyl chloride, pyridine, 0°C; iii) acetyl chloride/acetic acid/$H_2O$, acetic acid (36% for 3 steps); iv) 7-chloro-7-deaza-6-iodo-purine, NaH, $CH_3CN$, 50°C (73%); v) $Pd(PPh_3)_4$, CuI, CsF, DMF, 100°C (60%); vi) S*n*$Bu_3Cl$, *tert*-butyllithium, THF, −78°C to −20°C (65%); vii) DBU, DABCO, DMF, 75°C; viii) 25% TFA/DCM (46% over 2 steps); ix) NaOMe/MeOH, (61%); x) DMTrCl, pyridine (68%); xi) $PCl[(OCH_2)_2CN]N(iPr)_2$, DIPEA, $CH_2Cl_2$ (79%).

A procedure was then followed that employed a combination of cesium fluoride and cuprous salts to enhance the reaction rate.[28] The use of $Cu^I$ and highly polar solvents (NMP or DMF) in the Stille reaction is well-documented. The rate accelerating effect of $Cu^I$ is attributed to a preliminary transmetallation reaction with the organostannane that generates a more reactive organo–copper intermediate. In addition, the $Bu_3SnCl$ by-product can be efficiently transformed into insoluble $Bu_3SnF$, which is easily removed from the reaction mixture by filtration. In our case, a high temperature was needed to consume all the starting material to give a respectable yield of **4** (60%). Formation of compound **5** was achieved by using a mixture of DABCO and DBU. Under these conditions partial deprotection of the *tert*-butyloxycarbonyl protecting group occurred. Therefore, the Boc-intermediate was not isolated but was fully deprotected by using a 25% solution of TFA in DCM. Deprotection of the toluoyl group was then performed by using a solution of NaOMe (0.5 M) in MeOH, which gave the free qA nucleoside (**6**) in 61% yield. It was crucial to purify this nucleoside by column chromatography in order to achieve successful tritylation in the next step. Purified compound **6** was tritylated by using dimethoxytrityl chloride in pyridine to give (**7**) in 68% yield. This was finally converted to the qA phosphoramidite monomer (**8**) in 79% yield.

### Spectroscopic characterisation of the qA monomer

*Steady state absorption and fluorescence spectra*: The steady state absorption and emission spectra of the quadracyclic adenine (qA) monomer excited at 337 nm in water and methanol are shown in Figure 2. The absorption spectrum is characterised by a sharp peak at 335 nm with an extinction coefficient of $5000\,M^{-1}cm^{-1}$ (in water) and a shoulder at 300 nm; this indicates the presence of several different transitions ($S_0 \rightarrow S_2$ and $S_0 \rightarrow S_3$, respectively, as discussed below) and a lower energy spectral feature above 370 nm. The absorption of qA at 335 nm is red-shifted compared to the natural nucleobases, which absorb up to 300 nm, and therefore allows for easy selective excitation. This is an advantage compared to, for example, the fluorescent triazole adenine,

  

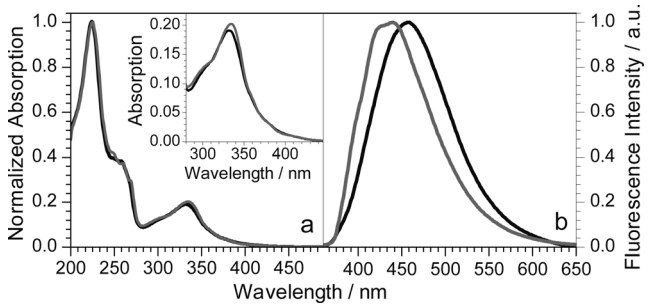


Figure 2. a) Normalised absorption, and b) emission spectra of the qA monomer in water (black) and methanol (grey) when excited at 337 nm at 25 °C. Inset: lowest energy absorption band of qA outside the region of DNA absorption.

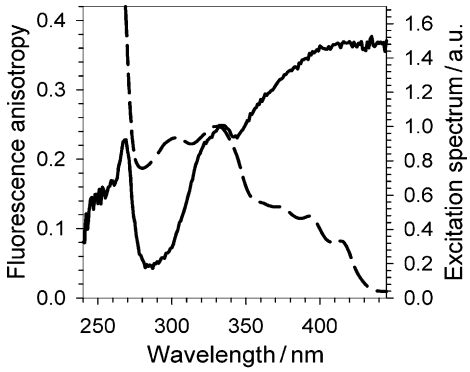


| Absorption transitions | Wavelength (nm) | Oscillator strength |
|---|---|---|
| $S_0$ - $S_1$ | 349.51 | 0.0594 |
| $S_0$ - $S_2$ | 329.84 | 0.1968 |
| $S_0$ - $S_3$ | 283.15 | 0.1049 |

Figure 3. Excitation anisotropy spectrum (black line) and excitation spectrum (dashed line) of qA in an $H_2O$/ethylene glycol matrix (1:2 mixture) at −100 °C. The table shows the results of the TDDFT calculations on the three lowest energy electronic transitions of qA.

$A^T$, ($\lambda_{abs,max}$ = 282 nm)[24] or the series of 7-substituted adenines designed by Seela et al., of which the most fluorescent members have their absorption centred around 280 nm.[29]

As can be seen in Figure 2 the two emission spectra of qA in water and methanol show a maximum emission peak at 456 and 440 nm, respectively. Furthermore, the spectral shape and position of the emission are independent of the excitation energy; this suggests that emission always occurs from the same energy level ($S_1$; see the Supporting Information). qA shows a lower fluorescence in water ($\Phi_f$ = 6.8 %, $\lambda_{ex}$ = 337 nm) than other fluorescent adenine analogues, such as 2-AP (68 %),[14] 6-MAP (39 %), DMAP (48 %),[9] xA (44 % in methanol),[11a] hxy$^7$c$^7$A$_d$ (27 %)[30] or triazole adenine (61 %).[24] However, as will be discussed below, qA is a promising FBA when located inside DNA.

*Transition dipole moments*: To obtain detailed information about the transition dipole moments of qA, we recorded the steady-state excitation spectrum and fundamental anisotropy of the qA monomer in an $H_2O$/ethylene glycol matrix (1:2 mixture) at −100 °C (Figure 3). As in the absorption spectrum recorded for the free monomer in solution (Figure 2), this excitation spectrum (Figure 3, dashed line) shows a sharp peak around 330 nm, a weaker one at 300 nm, and a longer wavelength absorption transition centred at 390 nm with fine structure due to the vibrational levels. The fundamental anisotropy, $r_0$ (Figure 3), shows three different main plateaus between 280 and 450 nm. The lowest energy plateau is located between 390 and 450 nm ($r_0$ = 0.36), the second occurs around the absorption maximum at 330 nm ($r_0$ = 0.25) and the third around 300 nm ($r_0$ = 0.05). The low energy plateau shows an $r_0$ value close to the theoretical maximum of 0.4. This suggests that, in this particular spectral region, the absorption and emission transition dipole moments are parallel.

The reason why this experimental value is slightly lower could be due to vibrational torsions and slight geometrical changes in the molecule between the moment of excitation and emission. Furthermore, as was mentioned in the previous section, all emission spectra of qA are virtually independent of the excitation wavelength; this suggests that the emission transition dipole moment is invariable over this spectral region (see the Supporting Information). As a result of this, the anisotropy recorded will give a direct measure of the angles between a certain absorption transition moment and the emission transition moment. Consequently, the three different plateaus mentioned above, suggest that there are three distinct absorption transition dipole moments: one around 400 nm that is parallel to the emission transition moment ($S_0 \rightarrow S_1$), and two others ($S_0 \rightarrow S_2$ and $S_0 \rightarrow S_3$, respectively) with different angles relative the constant emission dipole moment. We also noticed a bulge located around the second plateau at 340 nm. This observation might be attributed to vibrational features situated between the electronic states $S_2$ and $S_1$.

Theoretical calculations of the lowest singlet energy excitations of qA were performed on the B3LYP/6-31G(d,p) optimised geometry by using TDDFT B3LYP/6-311+G(2d) including a CPCM solvation shell for $H_2O$ as implemented in Gaussian 03. Above 280 nm these calculations show three significant transitions centred at 283.15 nm ($f$ = 0.1049; $S_0 \rightarrow S_3$), 329.84 nm ($f$ = 0.1968; $S_0 \rightarrow S_2$) and 349.51 nm ($f$ = 0.0594; $S_0 \rightarrow S_1$). Comparing these values to the transitions suggested by the absorption and excitation spectra as well as the fundamental anisotropy, we observe that they match very well, except that they are somewhat blue-shifted. This kind of spectral shift between theoretical calculations and experiments is common and has also been observed for other FBAs.[12a,31] Importantly, the relative positions of the transitions and the trend in the calculated oscillator strengths correspond very well to the intensity of the spectral bands of both the absorption and excitation spectra of the qA mono-

  

mer. This is further evidence for the existence of three different transitions in the low energy band of qA.

*Fluorescence properties of qA*: The fluorescence quantum yields of qA obtained for different excitation wavelengths between 295 and 377 nm are shown in Figure 4. Surprisingly

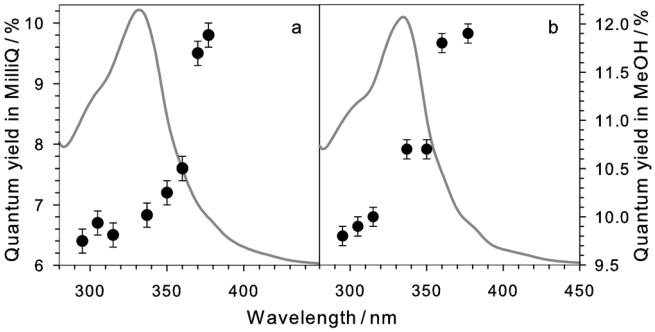


Figure 4. Steady-state absorption spectrum and fluorescence quantum yields of qA for different excitation wavelengths between 295 and 377 nm in: a) MilliQ water, and b) methanol. All measurements were performed at 25(±0.5) °C.

the fluorescence quantum yields in water decrease gradually from 9.8 to 6.4% with excitation at shorter wavelengths (see the Supporting Information). When exciting at wavelengths further into the red region even higher quantum yields are detected. However, these values are difficult to accurately determine since the excitation energy severely overlaps the emission spectrum at these wavelengths. Nevertheless, irrespective of the excitation wavelength the spectral envelope of the emission and its position stays virtually the same for the monomer both in water and in methanol (see the Supporting Information). Furthermore, the time-resolved fingerprint of qA in water is defined by a single time component of 3.2 ns ($\chi^2 = 1.684$), which is insensitive to excitation (295, 330 and 377 nm) and emission wavelengths (456 and 520 nm; see the Supporting Information). This suggests that regardless of which state is being populated upon excitation, the fluorescence always originates from deactivation of the same electronic state ($S_1$). Thus, internal conversion from the high-energy electronic states ($S_2$, $S_3$) occurs followed by a deactivation of the excited $S_1$ population through fluorescence or non-radiative processes.

The decrease in quantum yield from 377 to 300 nm is stepwise in methanol (Figure 4b) and more continuous in water (Figure 4a); this suggests a gradually changing overlap between the electronic transitions $S_0 \rightarrow S_3$, $S_0 \rightarrow S_2$ and $S_0 \rightarrow S_1$. This indicates a more efficient non-radiative deactivation to the ground state when populating the $S_2$ or $S_3$ states rather than the $S_1$ state. The highest quantum yield value is obtained when mostly populating the $S_1$ state ($\lambda_{exc} = 377$ nm); when the population ratio is increased between $S_2$ and $S_1$ (i.e., exciting at lower wavelengths) the quantum yield decreases. Upon excitation further into the blue to $S_3$ ($\lambda_{exc} = 295$ nm) the fluorescence quantum yield in water does not change significantly (6.8 and 6.4%, respectively). To explain these observations we suggest a hypothesis in which part of the highly excited population could relax and then be trapped in a non-radiative parasite state. Such an energy trap state could be localised between the $S_2$ and $S_1$ states. Indeed, the decrease in quantum yield of at least 30% between the $S_1$ and $S_2$ states clearly indicates that a decrease of deactivation from $S_1$ through the fluorescence path occurs. In conclusion, we suggest a deactivation pathway of the qA monomer in which at least 30% of the molecules that are excited to higher electronic states ($S_2$, $S_3$) get trapped in a "parasite state" and the rest relax to the lowest vibrational level of $S_1$ and then further to $S_0$ by emission or internal conversion and vibrational relaxation. It has been observed that the quantum yield of the virtually non-fluorescent natural mononucleotide, dGMP, also varies with the excitation energy. In that case, populating higher energy electronic states was suggested to open non-radiative deactivation pathways.[32]

## Structure and stability of DNA duplexes containing qA

*UV duplex melting experiments*: In order to investigate the spectroscopic and structural properties of qA inside DNA, eleven 10-mer oligonucleotides were synthesised, each with one qA base incorporated opposite T (Table 1). To evaluate the effect of both purines and pyrimidines neighbouring qA at the 3′ and 5′ ends, these eleven sequences have variations in the bases directly flanking qA. Furthermore, we designed a twelfth 10-mer DNA duplex containing two qA molecules in order to investigate the structural influence and the photophysical properties of qA in this case (sequence *CT*,*T***A**).

The melting temperatures of the different duplexes containing qA ($T_m^{qA}$) as well as those of the corresponding nat-

Table 1. Melting temperatures of the qA modified DNA duplexes ($T_m^{qA}$). Melting temperatures of the corresponding natural duplexes are also listed ($T_m^{A}$) as well as the corresponding difference in melting temperature with the modified duplexes ($\Delta T_m$).

| DNA sequence[a,b] | Neighbouring bases[c] | $T_m^{qA}$ [°C][d] | $T_m^{A}$ [°C][d] | $\Delta T_m$ [°C] |
|---|---|---|---|---|
| 5′-d(CGCAA(**qA**)ATCG)-3′ | **AA** | 46.3 | 46.6 | −0.3 |
| 5′-d(CGCAG(**qA**)ATCG)-3′ | **GA** | 48.3 | 48.3 | 0.0 |
| 5′-d(CGCAG(**qA**)GTCG)-3′ | **GG** | 51.9 | 51.5 | 0.4 |
| 5′-d(CGCAG(**qA**)CTCG)-3′ | **G***C* | 52.3 | 50.8 | 1.5 |
| 5′-d(CGCAA(**qA**)CTCG)-3′ | **A***C* | 52.7 | 50.8 | 1.9 |
| 5′-d(CGCAT(**qA**)ATCG)-3′ | ***T*A** | 48.5 | 45.3 | 3.2 |
| 5′-d(CGCAC(**qA**)ATCG)-3′ | ***C*A** | 53.2 | 49.9 | 3.3 |
| 5′-d(CGCAT(**qA**)GTCG)-3′ | ***T*G** | 48.7 | 45.3 | 3.4 |
| 5′-d(CGCAC(**qA**)CTCG)-3′ | *CC* | 58.2 | 52.9 | 5.3 |
| 5′-d(CGCAC(**qA**)TTCG)-3′ | *CT* | 56.1 | 49.6 | 6.5 |
| 5′-d(CGATT(**qA**)TGCG)-3′ | *TT* | 50.6 | 43.7 | 6.9 |
| 5′-d(CGC(**qA**)T(**qA**)ATCG)-3′ | *CT*,***T*A** | 55.6 | 46.4 | 9.2 |

[a] The natural sequences contain an adenine instead of (qA). [b] Duplexes were obtained by annealing the sequences listed to their natural complementary oligonucleotides. [c] Sequences are named by the bases neighbouring qA, in which the purines are shown in bold and the pyrimidines in italic. [d] Samples were prepared in phosphate buffer (pH 7.5, 200 mM $Na^+$, 17 mM phosphate).

  

ural duplexes ($T_m^A$) are listed in Table 1. In general qA has a stabilising effect on the duplex structure, which translates to an average rise in melting temperature of approximately 3 °C. Moreover, the extent of this stabilisation is dependent on the bases flanking qA, which allows for selecting the desired stability of a qA-containing duplex. When qA is flanked by two purines (**AA**, **GA** and **GG**), the stability of the duplex structure on average is equal to that of the natural duplexes. A pyrimidine flanking qA on the 3′ side (**G***C* and **A***C*) causes a slight stabilisation of the duplexes (1.7 °C on average), whereas a pyrimidine neighbouring on the 5′ side (*T***A**, *C***A** and *T***G**) causes a moderate stabilisation (3.3 °C on average). DNA duplexes containing qA flanked by two pyrimidines have the highest stability (*CC*, *CT* and *TT*), which is shown by an average rise in melting temperature of 6.2 °C compared to the natural duplexes. In general we can conclude that the stability of the duplexes is increased most when qA is flanked by a pyrimidine on the 5′ side.

When investigating the structural overlap of qA and its neighbours in sequences *C***A** and *CC*, an overlap between the extended ring system of qA and the cytosine flanking it on the 5′ side is observed. This overlap is not present for natural adenine in the same sequence (data not shown). The increased overlap arising when qA instead of natural A is flanked by a pyrimidine on the 5′ side might explain the higher stability of such duplexes. The overall stabilising effect of qA can thus be explained by better π–π stacking with its neighbours due to the extended ring system compared to natural adenine. Furthermore, the additional rings extended on C6 and N7 of adenine are well accommodated in the major groove in contrast to extensions on the C8-position, which are known to destabilise the duplex structure.[24,33] It should also be noted that sequence *CT*,*T***A** containing two qAs shows a rise in melting temperature (9.2 °C) that is virtually equal to the linear combination of the stabilisations caused by qA in the sequences *CT* and *T***A** (9.7 °C).

The UV melting results determined for qA are very similar to earlier observations for the tricyclic cytosine analogues tC and tC$^O$, containing a similar two-ring extension towards the major groove.[12a,34] Both tC and tC$^O$ increase the melting temperature of 10-mer duplexes by about 3 °C under similar conditions (phosphate buffer, pH 7.5, [$Na^+$] = 50 mM). Furthermore, as for qA, the most stable duplexes are formed when they are flanked by a pyrimidine on the 5′ side. Also in the case of tC and tC$^O$, a better overlap between the extended ring systems and the adjacent 5′ pyrimidine has been suggested as the reason for the increased duplex stability.[12a,34]

Importantly, qA is a good adenine analogue since it causes no destabilisation of the DNA structure. On the contrary, it slightly stabilises the duplexes depending on the neighbouring bases. This property distinguishes qA from most other fluorescent base analogues. For example, the widely used adenine analogue 2-aminopurine (2-AP) has been shown to cause a destabilisation of 10 °C in 10-mer duplexes (100 mM KCl, 0.1 mM EDTA, 21 μM DNA duplexes, decamer).[15b] Also, another study involving 14-mer duplexes confirmed the destabilising effect of 2-AP by a drop in melting temperature of 6 °C (15 mM sodium citrate, pH 7.25, 50 μM DNA duplexes).[15a] However, other studies have reported a more limited destabilisation of duplexes due to incorporation of 2-AP.[17,35] Besides 2-AP, other adenine analogues, such as the size-expanded adenine analogue xA, cause a destabilisation of 4.2–4.9 °C when centrally substituted into 12-mer duplexes (100 mM NaCl, 10 mM $MgCl_2$, 10 mM Na·PIPES, pH 7.0, 5.0 μM DNA).[11c] Also, the pteridine adenine analogues, 6MAP and DMAP, on average have shown a slight (2.4 °C) to moderate destabilisation (4.6 °C) in 21-mer duplexes (10 mM NaCl, 10 mM Tris, pH 7.5), respectively.[9] Furthermore, another purine analogue, the pteridine guanine analogue 3-MI, shows an average drop in melting temperature of 8.3 °C, which is comparable to a single base mismatch under similar conditions.[10b] As for qA, the modified 7-deaza-adenine analogues developed by Seela et al. have also been shown to stabilise DNA duplexes.[30,36] However, to the best of our knowledge, no reports have been published regarding the fluorescence properties of these analogues inside DNA.

*Circular dichroism*: CD spectra of the samples listed in Table 1 were used to evaluate any structural perturbations to the B-DNA helix caused by the incorporation of qA (Figure 5). All duplexes show a typical B-DNA signature, which in the region between 180 and 300 nm, is characterised by a positive band at 275 nm, a negative band at 240 nm, a band that is less negative or positive at 220 nm and a narrow negative band in the region between 220 and 190 nm, preceded by a large positive peak at 180–190 nm. Surprisingly there is no specific signal corresponding to the lowest energy absorption band of qA centred around 337 nm. For other common base analogues, such as tC or 2-

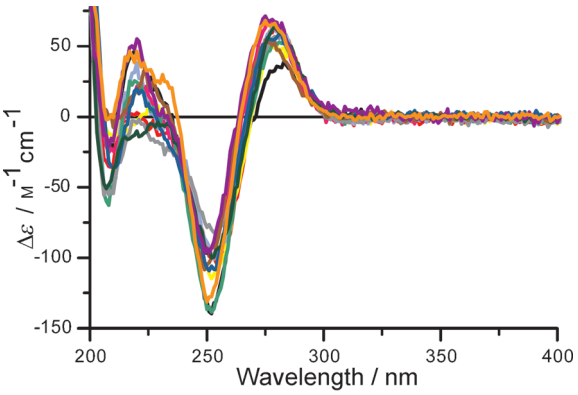


Figure 5. CD spectra of the twelve qA modified duplexes. Duplexes are named as the bases neighbouring qA (purines are shown in bold and pyrimidines in italic): **AA** (black), **GG** (red), **GA** (yellow), *CT* (light blue), *T***G** (pink), **A***C* (light green), *CC* (grey), *T***A** (brown), *C***A** (dark blue), **G***C* (dark green), *CT*/*T***A** (violet) and *TT* (orange). Duplexes were prepared at a concentration of 2.5 μM in phosphate buffer (pH 7.5, 200 mM $Na^+$, 17 mM phosphate) and measured at 25 °C; M on the Δε axis refers to the qA/duplex concentration (2.5 μM).

aminopurine, a CD band appears for the low energy transition.[34–35] However, similar observations to those made here for qA have been reported for the structurally comparable cytosine analogue $tC^O$.[12a] We have not yet found a satisfactory explanation for this phenomenon.

The CD signatures of all the modified duplexes containing qA were compared to those of the corresponding non-modified duplexes, and were shown to be virtually identical (see the Supporting Information). Overall it can be concluded that the incorporation of one or several qA molecules preserves the overall B-DNA structure.

*Base pairing specificity of qA*: To investigate the base-pairing specificity of qA, we synthesised oligonucleotides to combine with three of the modified sequences (**GA**, *CT* and *T***A**) to produce duplexes containing an adenine, guanine or cytosine instead of thymine opposite to qA. The sequences were chosen to evaluate the influence of having purines, pyrimidines or a combination of both directly neighbouring mismatched qA. The melting temperatures of the modified as well as the unmodified mismatched duplexes are listed in Table 2. For comparison, the melting temperatures of the matched duplexes with qA and A opposite to thymine are also shown. When comparing the difference in melting temperature between the modified matched and mismatched duplexes ($T_m^{qA-T}$ and $T_m^{qA-X}$) all three sequences are significantly destabilised when qA is placed opposite to G, C or A instead of thymine. This indicates that qA exhibits selective base-pairing with thymine, and hence, is a specific adenine analogue. In contrast, a less specific base-pairing pattern has been reported for other fluorescent base analogues. The adenine analogues 2-AP and triazole adenine, $A^T$, for example, are able to form stable base pairs with cytosine and adenine, respectively, besides the conventional base pairing with thymine.[16,24] Furthermore, the base discriminating fluorescent analogue BPP can form stable base pairs both with adenine and guanine.[4]

Interestingly, qA and natural adenine show the same order of preference for base-pairing partners. When comparing the destabilisations in Table 2, both for qA and A, a more stable mismatch is formed with guanine compared to the mismatches with cytosine and adenine. The same order of thermal stability has been reported before in a study by Gaffney and Jones for mismatches in a 9-mer oligonucleotide.[37] The fact that qA shows the same base pairing preference as natural adenine is an important indication that the base-pairing pattern upon modification with qA is indeed unperturbed.

The quantum yields of the duplexes containing a qA mismatch as well as the corresponding matched duplexes are listed in Table 3. On average the quantum yield increases threefold for the mismatched sequences compared to the matched qA–T sequences. We have observed that the average quantum yield of qA in single strands is higher or virtually equal to their corresponding mismatched duplexes. Thus, we suggest that the increase in quantum yield might be due to the weaker base-pairing between qA and the mismatching bases. This will lead to less rigid or less extensive base-stacking and an increased opening rate for the mismatched qA base pairs relative to qA–T. In spite of these perturbations, the CD spectra of the modified mismatched and matched duplexes are virtually identical (data not shown); this indicates that the overall B-DNA structure remains unchanged in these mismatched 10-mers.

Table 2. Melting temperatures of sequences containing quadracyclic adenine ($T_m^{qA-X}$) and natural adenine ($T_m^{A-X}$) opposite to guanine, adenine or cytosine (X). Melting temperatures of matched sequences with qA ($T_m^{qA-T}$) and A ($T_m^{A-T}$) are compared with the mismatched cases.

| Seq.[a] | X[b] | $T_m^{qA-T}$ [°C][c] | $T_m^{qA-X}$ [°C][c] | $\Delta T_m^{qA}$ [°C] | $T_m^{A-T}$ [°C][c] | $T_m^{A-X}$ [°C][c] | $\Delta T_m^{A}$ [°C] |
|---|---|---|---|---|---|---|---|
| | G | | 38.8 | 9.5 | | 35.6 | 12.4 |
| **GA** | A | 48.3 | 34.2 | 14.1 | 48.3 | 32.7 | 15.4 |
| | C | | 34.1 | 14.2 | | 28.7 | 19.3 |
| | G | | 47.6 | 8.5 | | 38.4 | 11.1 |
| *CT* | A | 56.1 | 40.5 | 15.6 | 49.6 | 33.1 | 16.4 |
| | C | | 39.3 | 16.8 | | 31.5 | 18.1 |
| | G | | 37.0 | 11.5 | | 31.2 | 12.4 |
| *T***A** | A | 48.5 | 33.5 | 15.0 | 45.3 | 27.3 | 16.3 |
| | C | | 32.8 | 15.8 | | 24.9 | 18.7 |

[a] Sequences are named by the bases neighbouring qA and A. Full sequences are listed in Table 1. [b] Base opposite qA or A in the mismatched sequences. [c] Samples containing duplexes (2.5 μM) were prepared in phosphate buffer (pH 7.5, 200 mM $Na^+$, 17 mM phosphate).

Table 3. Quantum yields of the mismatched ($\Phi^{qA-X}$) and matched ($\Phi^{qA-T}$) modified duplexes.

| Seq.[a] | X[b] | $\Phi^{qA-T}$ [%][c,d] | $\Phi^{qA-X}$ [%][c,d,e] |
|---|---|---|---|
| | G | | 3.0 |
| **GA** | A | 0.5 | 1.6 |
| | C | | 1.6 |
| | G | | 0.5 |
| *CT* | A | 0.2 | 0.5 |
| | C | | 0.5 |
| | G | | 0.4 |
| *T***A** | A | 0.2 | 0.5 |
| | C | | 0.4 |

[a] Sequences are named by the bases neighbouring qA and A. Full sequences are listed in Table 1. [b] Base opposite of qA or A in the mismatched sequences. [c] Samples containing duplexes (2.5 μM) were prepared in phosphate buffer (pH 7.5, 200 mM $Na^+$, 17 mM phosphate). [d] Fluorescence quantum yields were determined relative to the reference quinine sulfate in 0.5 M $H_2SO_4$ ($\Phi = 0.55$) at 25 °C, and are averages of at least two independent measurements. [e] Fluorescence quantum yields determined at 13 °C were very similar (maximum 11 % difference) to values presented here.

**Spectroscopic and photophysical characterisation of qA in DNA**: The fluorescence quantum yields and lifetimes of qA incorporated into the twelve single-stranded sequences, as

  

Table 4. Fluorescence quantum yields and average fluorescence lifetimes of the twelve single- and double-stranded oligonucleotides containing qA, referred to as ss and ds, respectively.

| Neighbouring $bases_{ss}$[a] | $\Phi_{f,ss}$ [%][b,c] | $\langle\tau\rangle_{ss}$ [ns][b,d] | Absorption $max_{ss}$ [nm][b] | Emission $max_{ss}$ [nm][b] | Neighbouring $bases_{ds}$[a] | $\Phi_{f,ds}$ [%][b,c] | $\langle\tau\rangle_{ds}$ [ns][b,d] | Absorption $max_{ds}$ [nm][b] | Emission $max_{ds}$ [nm][b] |
|---|---|---|---|---|---|---|---|---|---|
| **AA** | 5.8 | 1.3 | 337 | 432 | **AA** | 0.6 | 0.7 | 334 | 434 |
| **GG** | 5.5 | 2.0 | 337 | 433 | **GG** | 0.6 | 0.9 | 336 | 435 |
| **GA** | 4.4 | 2.0 | 337 | 432 | **G***C* | 0.6 | 1.4 | 339 | 453 |
| **A***C* | 2.0 | 0.6 | 338 | 434 | **GA** | 0.5 | 0.5 | 336 | 438 |
| **G***C* | 1.6 | 1.3 | 337 | 438 | ***C*A** | 0.3 | 0.5 | 337 | 444 |
| ***C*A** | 1.0 | 0.8 | 338 | 433 | ***CT*,*T*A** | 0.3 | 1.3 | 337 | 457 |
| ***T*A** | 0.6 | 0.7 | 338 | 434 | **A***C* | 0.2 | 0.4 | 337 | 441 |
| ***CT*,*T*A** | 0.4 | 0.6 | 337 | 439 | ***T*A** | 0.2 | 0.6 | 337 | 451 |
| ***T*G** | 0.4 | 0.6 | 337 | 437 | ***T*G** | 0.2 | 0.6 | 334 | 453 |
| *CC* | 0.4 | 0.4 | 338 | 440 | *CT* | 0.2 | 1.3 | 331 | 459 |
| *CT* | 0.3 | 0.5 | 337 | 443 | *CC* | 0.2 | 0.8 | 337 | 452 |
| *TT* | 0.2 | 0.7 | 338 | 434 | *TT* | 0.2 | 0.7 | 336 | 452 |

[a] Full sequences are listed in Table 1. [b] Samples were prepared in phosphate buffer (pH 7.5, 200 mM $Na^+$, 17 mM phosphate). [c] Fluorescence quantum yields were determined relative to the reference quinine sulfate in 0.5 M $H_2SO_4$ ($\Phi_f = 0.55$) at an excitation wavelength of 337 nm at 25 °C, and are averages of three independent measurements. [d] Fluorescence decays were recorded by using an excitation wavelength of 330 nm and monitoring emission at 456 nm. For each sample, two independent measurements were obtained to confirm the reproducibility of the results. Decays were convoluted by using the IRF and fitted to a bi- or tri-exponential function. Detailed fitting parameters are presented in the Supporting Information.

well as the corresponding duplexes are listed in Table 4. Also, the absorption and emission maxima of each sequence are presented. The emission maxima of qA in both single- and double-stranded sequences (except duplexes *CT* and *CT*,*T***A**) show a blue-shift compared to the free qA monomer in water ($\lambda_{em,max} = 456$ nm). This is according to expectations upon introducing qA to a less polar environment since TDDFT calculations suggest an increased dipole moment in the excited state.[38] Furthermore, slight variations for single-stranded samples (432–443 nm) and large shifts (434–459 nm) for duplexes can be observed between various sequences. In contrast, the absorption maxima are virtually the same for all single-stranded sequences (337–338 nm) and only slightly red-shifted compared to the free qA monomer ($\lambda_{abs,max} = 335$ nm). For the modified duplexes these numbers show more variation, and range from 331 to 339 nm, with slight red-shifts (except sequences *CT*, **AA** and *T***G**) compared to the qA monomer. Similar observations have been made for the FBAs 2-AP[14] and 3-MI.[8] Moreover, red-shifts are common for intercalating dyes, such as YO, YOYO[39] and ethidium bromide.[40]

A general decrease in the quantum yields and average fluorescence lifetimes are observed upon incorporation of qA into oligonucleotides. The extent of the decrease is highly dependent on the immediately surrounding bases (vide infra). Lifetimes of qA inside DNA were fitted to two or three exponentials, for which detailed fitting parameters are shown in the Supporting Information. The average lifetimes of qA vary between 0.4–2.0 ns in single strands and between 0.4–1.4 ns in duplexes (Table 4). The average lifetimes for all single- and double-stranded molecules (1.0 and 0.8 ns, respectively) are approximately three- and four-times shorter, respectively, than the lifetime of the qA monomer in water ($\tau = 3.2$ ns; $\chi^2 = 1.684$). The observed general decreases in quantum yield and average lifetime upon incorporation into DNA are common features of most fluorescent base analogues.[2a,6,10a,14,24] A range of theories have been suggested in the literature to explain this phenomenon. It has previously been shown that, for example, in single-stranded systems, the base-stacking effect could produce significant charge transfer by the molecular orbital overlap with the surrounding natural bases.[41]

In the double-stranded structure there is also the effect of the opposite strand to consider. Particularly in the case of 2-AP, the results of Ward et al. suggest that this quenching could be due to base-pairing.[14] Another explanation for the decrease in fluorescence intensity and the shortening of fluorescence lifetimes in a DNA-context could be the improved accessibility of a conical intersection (CI) between the excited state and the ground state[42] induced by the immediate surroundings in the DNA. It has been proven that such CIs occur in all natural nucleobases and in various fluorescent base analogues,[43] such as 2-AP.[44] Even though this hypothesis needs to be verified by theoretical calculations on qA, it is possible that in the monomeric form, the CI between $S_1$ and $S_0$ is not accessible to the excited population because of energy barriers that occur on the potential energy surface. These energy barriers could disappear when qA is incorporated into DNA systems, and thus a larger part of the excited population could relax non-radiatively through the CI. This kind of mechanism could explain the short time-components found here in the fitting parameters (see the Supporting Information).

An average decrease in fluorescence quantum yield of elevenfold was observed upon incorporation of the qA monomer ($\Phi_{water,\lambda ex337\,nm} = 6.8\,\%$) into single-stranded DNA (Table 4). Moreover, qA shows a further sensitivity to its microenvironment as the quantum yields, average lifetimes and emission maxima of the sequences differ substantially depending on the bases neighbouring qA. As can be observed in Table 4, qA shows the highest quantum yield in oligonucleotides when it is surrounded by two purines (**AA**, **GG**, **GA**), followed by the group of sequences with only one purine neighbouring qA at the 5′ side (**A***C*, **G***C*) and by the

  

group with one purine on the 3′ side (*C***A**, *T***A**, *T***G**). The lowest quantum yield values were recorded for the group of sequences (*CC*, *CT* and *TT*) with two pyrimidines flanking qA.

For the corresponding duplexes, a further fourfold decrease in average quantum yields can be observed compared to the single-stranded sequences (Table 4). Also, shorter average lifetimes were observed for half of the sequences (**AA**, **GG**, **GA**, **A***C*, *C***A** and *T***A**). As for single strands, the highest quantum yield values were observed among the group of sequences with two purines flanking qA (**AA**, **GG**, **GA**). The **G***C* sequence can also be found among the higher values, but all other double-stranded sequences show lower and similar quantum yields (0.2–0.3%). It should be noted that duplexes (**AA**, **GG** and **GA**) with two purines flanking qA, having the same stability as natural duplexes, are the sequences that on average show the highest quantum yield both in single- and double-stranded DNA. In contrast, sequences *CC*, *TT* and *CT* are the sequences that have the highest duplex stability and the lowest quantum yields. This can indicate a more firm stacking of qA with the neighbouring bases in the latter sequences, and hence explain an increased quenching efficiency.

The fact that **GG** is one of the sequences with the highest quantum yield is in stark contrast to observations made for the majority of fluorescent base analogues. Guanine is the natural base with the lowest oxidation potential and, thus, the highest susceptibility to oxidation.[45] This means that, depending on the oxidation potential of the neighbouring base analogue, G can transfer an electron into it, thereby quenching the excited state by photo-induced electron transfer (PET). For several common base analogues, such as the adenine analogues 2-aminopurine,[41c] triazole adenine,[24] the cytosine analogue $tC^{O}$[12a] and the base-discriminating analogue BPP,[4] a decreased quantum yield has been observed due to neighbouring guanines. It has also been suggested that the pteridine analogues 6MAP, DMAP and 3MI, act as excited state acceptors, which are preferentially quenched by purines.[46] We have not measured the redox potentials of qA and therefore cannot draw any conclusions regarding possible PET. One should remember though that even if the redox potential of qA had been determined, structural parameters, such as stacking with neighbouring bases and relative orientation, are also expected to play an important role for PET. Thus, knowledge of the redox potential of the qA monomer would give a clue to possible PET but could not tell the full story. However, as for many other FBAs we believe the quenching of qA inside DNA to be due to a combination of various mechanisms, all influenced by the surrounding sequence and base stacking. Therefore, we are currently investigating the details of the reduced lifetimes using a range of time-resolved techniques to obtain a more complete picture about the complex quenching mechanisms.

Importantly, qA shows significant fluorescence inside DNA compared to other adenine analogues. The maximum quantum yield value reached in single strands (5.8%) is approximately four-times higher than corresponding values recorded for nucleic acids containing 2-AP,[14] and also slightly higher compared to 6MAP.[9] In double-stranded DNA the maximum value recorded for qA (0.6%) is comparable to that of 2-AP.[14] The fluorescence decays of single- and double-stranded systems containing qA, just as for 6-MAP and DMAP, show more complex fitting parameters, and the dominant time component of those decays is shorter than that of the free monomer itself.[9] Furthermore, we recorded fluorescence melting curves for duplex **AA**; this yielded a virtually identical melting temperature to that recorded with UV/Vis melting ($T_{m,UV}=46.3\,°C$; $T_{m,F}=46.8\,°C$). This indicates no pre-melting at the qA-modified site and illustrates the applicability of qA as a fluorescent thymine-specific and non-perturbing adenine analogue.

## Conclusion

In conclusion, quadracyclic adenine, qA, is an environment-sensitive non-perturbing fluorescent adenine analogue. The analogue is easy to selectively excite because its lowest energy excitation maximum (335 nm) is well resolved from the natural DNA absorption. Surprisingly, the quantum yield of qA varies with excitation energy, despite the fact that its emission always occurs from the $S_1$ state. The free monomer of qA is moderately fluorescent ($\Phi_{water,\lambda ex337\,nm}=6.8\%$) in comparison with other adenine analogues, but upon incorporation into oligonucleotides it reaches quantum yield values of up to four-times higher than corresponding values recorded for 2-AP. Furthermore, inside double-stranded DNAs the quantum yield of qA is of the same order as 2-AP in duplex systems.[14] Most importantly, the DNA duplex stability is either enhanced or preserved depending on the bases flanking qA. This is in contrast to the destabilisation caused by other fluorescent adenine analogues, such as 2-AP, 6MAP, DMAP, xA or triazole adenine, and is therefore a promising feature.[9,11c,14,24] To the best of our knowledge these properties of qA are unprecedented for fluorescent adenine analogues. Additionally, the highly selective base pairing between qA and thymine is an advantageous feature for many purposes. For the most common adenine analogue 2-AP and also for the recently developed triazole adenine, a lack of specificity has been reported.[14,24] In combination, these favourable properties of qA make it an interesting alternative to 2-AP in fluorescent experiments that require detailed measurements and a need to maintain the integrity of the DNA double helix. As a result of the promising properties found here, several derivatives of qA are currently being synthesised, and are aimed at even higher quantum yields but maintain the important ability to form stable duplexes and specific pairing with thymine.

## Experimental Section

**General**: The synthesis route to the quadracyclic adenine monomer is presented in the results section (Scheme 1). Detailed synthesis proce-

  

dures, compound characterisation, incorporation of qA into oligonucleotides and purification of oligonucleotides are described in Scheme S1 in the Supporting Information.

**Sample preparation**: DNA samples were prepared in sodium phosphate buffer (pH 7.5, 200 mM $Na^+$, 17 mM phosphate) and their concentrations were determined by recording the absorption at 260 nm. The extinction coefficients of the various sequences were calculated by summation of the extinction coefficients of the individual natural bases and qA. This sum was multiplied by 0.9 to correct for base stacking interactions. The extinction coefficient of qA was determined to be $10000\,M^{-1}cm^{-1}$ at 260 nm in water. This was obtained by measuring the absorption of a solution with a known concentration (86.4 μM) of qA. The extinction coefficients that were used for the different bases at 260 nm were $\varepsilon_T = 9300$, $\varepsilon_C = 7400$, $\varepsilon_G = 11800$, $\varepsilon_A = 15300$ and $\varepsilon_{qA} = 10000\,M^{-1}cm^{-1}$. From these extinction coefficients, those for the different modified sequences were calculated to be: $\varepsilon_{\mathbf{GA}} = 96800$, $\varepsilon_{CT} = 87400$, $\varepsilon_{\mathbf{GC}} = 89600$, $\varepsilon_{\mathbf{CA}} = 92800$, $\varepsilon_{\mathbf{GG}} = 93600$, $\varepsilon_{CC} = 85700$, $\varepsilon_{T\mathbf{A}} = 94500$, $\varepsilon_{\mathbf{AA}} = 99900$, $\varepsilon_{\mathbf{AC}} = 92800$, $\varepsilon_{T\mathbf{G}} = 91400$, $\varepsilon_{TT} = 93100$ and $\varepsilon_{CT,T\mathbf{A}} = 103500\,M^{-1}cm^{-1}$. Extinction coefficients of the unmodified oligonucleotides were calculated in the same way.

**UV and fluorescence melting experiments**: Samples containing modified duplex DNA (2.5 μM) were prepared by mixing buffered solutions containing the single-stranded complementary strands, of which the non-modified strand was in 15% excess. The excess was to assure hybridisation of all the modified strands for further fluorescence measurements. For natural DNA duplexes, the same procedure was applied by using equimolar amounts of single-stranded DNA. For UV melting experiments, duplex samples were heated to 90°C, and annealed by being cooled to 5°C at the rate of $1\,°C\,min^{-1}$. Next, melting curves were recorded during heating of the samples to 90°C, followed by cooling to 5°C at a rate of $0.5\,°C\,min^{-1}$. The temperature was kept at 90°C for 5 min between heating and cooling. The melting curves were measured on a Varian Cary 4000 spectrophotometer with a programmable multi-cell temperature block by using an absorption wavelength of 260 nm. Melting temperatures were calculated by using the half maximum and the maximum of the first derivative of the melting curves. The values presented in this paper are averages of at least two independent measurements. The fluorescence melting curves for duplex **AA** were recorded on a Varian Cary Eclipse instrument. Samples were annealed by being heated to 90°C, followed by cooling to 15°C at a rate of $0.5\,°C\,min^{-1}$. Next, melting curves were recorded while the samples were heated to 90°C, followed by cooling to 15°C also at a rate of $0.5\,°C\,min^{-1}$. The melting temperature was calculated as the maximum of the first derivative of the melting curve.

**Circular dichroism**: CD spectra of 2.5 μM duplex samples, which were prepared as described above, were recorded on a Chirascan CD spectrophotometer. The spectra were recorded at 25°C for a wavelength range of 200 to 420 nm. Corrections for background contributions were made and final spectra are averages of at least five measurements at a scan rate of $2\,nm\,s^{-1}$.

**Fluorescence measurements**

*Steady state fluorescence measurements*: For all steady-state fluorescence measurements, a SPEX fluorolog 3 spectrofluorimeter (JY Horiba) was employed. Buffered solutions of qA-modified DNA duplexes were prepared as described above (pH 7.5, 200 mM $Na^+$, 17 mM phosphate). Samples containing the monomer in Milli-Q water or in methanol and buffered solutions of single-stranded modified oligonucleotides were set to an absorption of approximately 0.03 at the excitation wavelength. Quantum yields were determined relative to the quantum yield of quinine sulfate ($\Phi_f = 0.55$) in $H_2SO_4$ (0.5 M) at 25°C.[47] For the duplexes and single-stranded oligonucleotides an excitation wavelength of 337 nm was used and emission spectra were recorded between 340 and 700 nm. The quantum yield of the qA monomer in Milli-Q water and methanol was recorded as a function of seven different excitation wavelengths between 295 and 377 nm. The emission of the quinine sulfate reference was recorded between 305 and 700 nm.

Steady-state excitation spectra were recorded by exciting between 240 and 450 nm and monitoring the emission fixed at 456 nm. Glan polarisers were used to obtain the polarised excitation spectra necessary to calculate the anisotropy, $r$, from Equation (1), in which the instrument correction factor is given by Equation (2) and nd $I_{XY}$ is the excitation spectrum for which the subscripts $X$ and $Y$ denote polarisation directions of the excitation and emission light, respectively, and H and V refer to horizontal and vertical, respectively.

$$r = \frac{I_{VV} - GI_{VH}}{I_{VV} + 2GI_{VH}} \tag{1}$$

$$G = \frac{I_{HV}}{I_{HH}} \tag{2}$$

The anisotropy of the immobile qA monomer in $H_2O$/ethylene glycol (1:2 mixture) glass at −100°C, also known as the fundamental anisotropy ($r_{0i}$) for a certain transition ($i$) is related to the angle between the absorbing and the emitting transition moments ($\alpha_i$) as given by Equation (3).

$$r_{oi} = \frac{1}{5}(3\cos^2\alpha_i - 1) \tag{3}$$

*Time-resolved fluorescence measurements*: Time-resolved fluorescence measurements were performed by using time-correlated single photon counting (TCSPC). The excitation source was the third harmonic (330 or 295 nm) of a Tsunami mode-locked Ti-sapphire laser running at 80 MHz. The UV pulses (1–2 ps) were generated in a Tsunami frequency tripler by using two 0.5 mm type I BBO crystals. The fluorescence of the samples was spectrally filtered at 456 nm by a monochromator and detected by a microchannel plate photomultiplier Hamamatsu R3809U-50. The counts were fed into a multichannel analyser with 4096 channels (Lifespec, Edinburgh Analytical Instruments) where a minimum of 10000 counts were recorded in the top channel. All fluorescence decays were recorded in a time window of 10 ns and the spectral resolution of the monochromator was set from 5 to 11 nm. The intensity data were convoluted with the instrument response function (IRF), the full width half maximum (FWHM) of which is given at 50 ps and fitted to two- or three-exponential expressions with the program Fluofit Pro v.4 (PicoQuant, GmbH) for the free monomer in solution and the modified single strands. For the modified duplexes, a fitting program created by Thomas Gustavsson from the Francis Perrin laboratory at CEA-Saclay was used. This uses a simple normalised analytical expression: $F(t) = \text{const} + a \times \exp(-t/t_1) + (1-a) \times b \times \exp(-t/t_2) + (1-a) \times (1-b) \times c \times \exp(-t/t_3) + (1-a) \times (1-b) \times (1-c) \times \exp(-t/t_4)$. To describe the fluorescence decays in a quantitative way, we performed a nonlinear fitting/deconvolution procedure using bi- and triexponential functions, convoluted with the IRF. The average decay time with $j = 1$, 2 or 3 is given by Equation ().

$$\langle\tau\rangle = \frac{\sum_{i=1}^{j} \alpha_i \tau_i}{\sum_{i=1}^{j} \alpha_i} \tag{4}$$

## Acknowledgements

This work was supported by the Swedish Research Council and Olle Engkvist Byggmästare Foundation. Furthermore, we would like to thank Thomas Gustavsson from the Francis Perrin Laboratory CEA-Saclay in France for the use of his software to fit the fluorescence decays of the modified duplexes.

[1] D. Onidas, D. Markovitsi, S. Marguet, A. Sharonov, T. Gustavsson, *J. Phys. Chem. B* **2002**, *106*, 11367–11374.
[2] a) L. M. Wilhelmsson, *Q. Rev. Biophys.* **2010**, *43*, 159–183; b) R. W. Sinkeldam, N. J. Greco, Y. Tor, *Chem. Rev.* **2010**, *110*, 2579–2619.
[3] S. Preus, K. Kilså, L. M. Wilhelmsson, B. Albinsson, *Phys. Chem. Chem. Phys.* **2010**, *12*, 8881–8892.

  

[4] A. Okamoto, Y. Saito, I. Saito, *J. Photochem. Photobiol. C* **2005**, *6*, 108–122.
[5] a) N. J. Greco, Y. Tor, *J. Am. Chem. Soc.* **2005**, *127*, 10784–10785; b) S. G. Srivatsan, Y. Tor, *J. Am. Chem. Soc.* **2007**, *129*, 2044–2053; c) S. G. Srivatsan, N. J. Greco, Y. Tor, *Angew. Chem.* **2008**, *120*, 6763–6767; *Angew. Chem. Int. Ed.* **2008**, *47*, 6661–6665; d) S. G. Srivatsan, H. Weizman, Y. Tor, *Org. Biomol. Chem.* **2008**, *6*, 1334–1338.
[6] D. A. Berry, K. Y. Jung, D. S. Wise, A. D. Sercel, W. H. Pearson, H. Mackie, J. B. Randolph, R. L. Somers, *Tetrahedron Lett.* **2004**, *45*, 2457–2461.
[7] a) F. Wojciechowski, R. H. E. Hudson, *J. Am. Chem. Soc.* **2008**, *130*, 12574–12575; b) R. H. E. Hudson, R. D. Viirre, Y. H. Liu, F. Wojciechowski, A. K. Dambenieks, *Pure Appl. Chem.* **2004**, *76*, 1591–1598.
[8] S. L. Driscoll, M. E. Hawkins, F. M. Balis, W. Pfleiderer, W. R. Laws, *Biophys. J.* **1997**, *73*, 3277–3286.
[9] M. E. Hawkins, W. Pfleiderer, O. Jungmann, F. M. Balis, *Anal. Biochem.* **2001**, *298*, 231–240.
[10] a) M. E. Hawkins, *Cell Biochem. Biophys.* **2001**, *34*, 257–281; b) M. E. Hawkins, W. Pfleiderer, F. M. Balis, D. Porter, J. R. Knutson, *Anal. Biochem.* **1997**, *244*, 86–95.
[11] a) A. T. Krueger, E. T. Kool, *J. Am. Chem. Soc.* **2008**, *130*, 3989–3999; b) H. B. Liu, J. M. Gao, E. T. Kool, *J. Am. Chem. Soc.* **2005**, *127*, 1396–1402; c) J. M. Gao, H. B. Liu, E. T. Kool, *J. Am. Chem. Soc.* **2004**, *126*, 11826–11831.
[12] a) P. Sandin, K. Börjesson, H. Li, J. Mårtensson, T. Brown, L. M. Wilhelmsson, B. Albinsson, *Nucleic Acids Res.* **2008**, *36*, 157–167; b) P. Sandin, L. M. Wilhelmsson, P. Lincoln, V. E. C. Powers, T. Brown, B. Albinsson, *Nucleic Acids Res.* **2005**, *33*, 5019–5025.
[13] K. Börjesson, S. Preus, A. H. El-Sagheer, T. Brown, B. Albinsson, L. M. Wilhelmsson, *J. Am. Chem. Soc.* **2009**, *131*, 4288–4293.
[14] D. C. Ward, E. Reich, L. Stryer, *J. Biol. Chem.* **1969**, *244*, 1228–1237.
[15] a) O. V. Petrauskene, S. Schmidt, A. S. Karyagina, I. I. Nikolskaya, E. S. Gromova, D. Cech, *Nucleic Acids Res.* **1995**, *23*, 2192–2197; b) D. G. Xu, K. O. Evans, T. M. Nordlund, *Biochemistry* **1994**, *33*, 9592–9599.
[16] a) S. M. Watanabe, M. F. Goodman, *Proc. Natl. Acad. Sci. USA* **1982**, *79*, 6429–6433; b) L. C. Sowers, Y. Boulard, G. V. Fazakerley, *Biochemistry* **2000**, *39*, 7613–7620; c) S. M. Law, R. Eritja, M. F. Goodman, K. J. Breslauer, *Biochemistry* **1996**, *35*, 12329–12337.
[17] A. Dallmann, L. Dehmel, T. Peters, C. Mugge, C. Griesinger, J. Tuma, N. P. Ernsting, *Angew. Chem.* **2010**, *122*, 6126–6129; *Angew. Chem. Int. Ed.* **2010**, *49*, 5989–5992.
[18] R. P. Bandwar, S. S. Patel, *J. Biol. Chem.* **2001**, *276*, 14075–14082.
[19] E. Deprez, P. Tauc, H. Leh, J. F. Mouscadet, C. Auclair, M. E. Hawkins, J. C. Brochon, *Proc. Natl. Acad. Sci. USA* **2001**, *98*, 10090–10095.
[20] K. E. Augustyn, K. Wojtuszewski, M. E. Hawkins, J. R. Knutson, I. Mukerji, *Biochemistry* **2006**, *45*, 5039–5047.
[21] P. Sandin, J. Tumpane, K. Börjesson, L. M. Wilhelmsson, T. Brown, B. Nordén, B. Albinsson, P. Lincoln, *J. Phys. Chem. C* **2009**, *113*, 5941–5946.
[22] a) S. D. Gilbert, C. D. Stoddard, S. J. Wise, R. T. Batey, *J. Mol. Biol.* **2006**, *359*, 754–768; b) J. F. Lemay, J. C. Penedo, R. Tremblay, D. M. J. Lilley, D. A. Lafontaine, *Chem. Biol.* **2006**, *13*, 857–868.
[23] C. A. Buhr, M. D. Matteucci, B. C. Froehler, *Tetrahedron Lett.* **1999**, *40*, 8969–8970.
[24] A. Dierckx, P. Dinér, A. H. El-Sagheer, J. D. Kumar, T. Brown, M. Grøtli, L. M. Wilhelmsson, *Nucleic Acids Res.* **2011**, *39*, 4513–4524.
[25] M. Hoffer, *Chem. Ber.* **1960**, *93*, 2777–2781.
[26] Z. Kazimierczuk, H. B. Cottam, G. R. Revankar, R. K. Robins, *J. Am. Chem. Soc.* **1984**, *106*, 6379–6382.
[27] J. M. Muchowski, M. C. Venuti, *J. Org. Chem.* **1980**, *45*, 4798–4801.
[28] S. P. H. Mee, V. Lee, J. E. Baldwin, *Angew. Chem.* **2004**, *116*, 1152–1156; *Angew. Chem. Int. Ed.* **2004**, *43*, 1132–1136.
[29] F. Seela, M. Zulauf, M. Sauer, M. Deimel, *Helv. Chim. Acta* **2000**, *83*, 910–927.
[30] F. Seela, M. Zulauf, *Chem. Eur. J.* **1998**, *4*, 1781–1790.
[31] S. Preus, K. Börjesson, K. Kilså, B. Albinsson, L. M. Wilhelmsson, *J. Phys. Chem. B* **2010**, *114*, 1050–1056.
[32] F. A. Miannay, T. Gustavsson, A. Banyasz, D. Markovitsi, *J. Phys. Chem. A* **2010**, *114*, 3256–3263.
[33] R. G. Eason, D. M. Burkhardt, S. J. Phillips, D. P. Smith, S. S. David, *Nucleic Acids Res.* **1996**, *24*, 890–897.
[34] K. C. Engman, P. Sandin, S. Osborne, T. Brown, M. Billeter, P. Lincoln, B. Nordén, B. Albinsson, L. M. Wilhelmsson, *Nucleic Acids Res.* **2004**, *32*, 5087–5095.
[35] N. P. Johnson, W. A. Baase, P. H. von Hippel, *Proc. Natl. Acad. Sci. USA* **2004**, *101*, 3426–3431.
[36] F. Seela, H. Thomas, *Helv. Chim. Acta* **1995**, *78*, 94–108.
[37] B. L. Gaffney, R. A. Jones, *Biochemistry* **1989**, *28*, 5881–5889.
[38] J. R. Lakowicz, in *Principles of Fluorescence Spectroscopy*, 3rd ed., Springer, New York, **2006**, pp. 205–235.
[39] A. Larsson, C. Carlsson, M. Jonsson, B. Albinsson, *J. Am. Chem. Soc.* **1994**, *116*, 8459–8465.
[40] M. J. Waring, *J. Mol. Biol.* **1965**, *13*, 269–282.
[41] a) J. N. Wilson, Y. J. Cho, S. Tan, A. Cuppoletti, E. T. Kool, *ChemBioChem* **2008**, *9*, 279–285; b) J. M. Jean, K. B. Hall, *Proc. Natl. Acad. Sci. USA* **2001**, *98*, 37–41; c) O. J. G. Somsen, v. A. Hoek, v. H. Amerongen, *Chem. Phys. Lett.* **2005**, *402*, 61–65.
[42] *Conical Intersections: Electronic Structure, Dynamics & Spectroscopy* (Eds.: W. Domcke, D. R. Yarkony, H. Köppel), World Scientific Publishing, **2004**.
[43] "Quantum Mechanical Studies of the Photophysics of DNA and RNA Bases": K. A. M. Kistler, S. Matsika, in *Challenges and Advances in Computational Chemistry and Physics, Vol. 7* (Ed.: T.-S. Y. Lee, D. M. York), Springer, Heidelberg (Germany), **2009**, pp. 285–339.
[44] a) S. Perun, A. L. Sobolewski, W. Domcke, *Mol. Phys.* **2006**, *104*, 1113–1121; b) J. X. Liang, S. Matsika, *J. Am. Chem. Soc.* **2011**, *133*, 6799–6808.
[45] S. Fukuzumi, H. Miyao, K. Ohkubo, T. Suenobu, *J. Phys. Chem. A* **2005**, *109*, 3285–3294.
[46] M. Narayanan, G. Kodali, Y. J. Xing, M. E. Hawkins, R. J. Stanley, *J. Phys. Chem. B* **2010**, *114*, 5953–5963.
[47] W. H. Melhuish, *J. Phys. Chem.* **1961**, *65*, 229–235.

Received: October 31, 2011
Published online: March 21, 2012

  